

Interface Between Alkylammonium Ions and Layered Aluminophosphates Materials: A Combined Theoretical and Experimental Study

Maddalena D'Amore,[†] Chiara Bisio,[†] Giovanni Talarico,[‡] Maurizio Cossi,^{*,†} and Leonardo Marchese^{*,†}

Dipartimento di Scienze e Tecnologie Avanzate, Centro Interdisciplinare Nano-SiSTE MI, Università del Piemonte Orientale “A. Avogadro”, Via Bellini 25/G, Alessandria, Italy, and Dipartimento di Chimica, “Paolo Corradini” Università di Napoli “Federico II”, Complesso Monte S. Angelo, Via Cintia, 80126 Napoli, Italy

Received April 4, 2008. Revised Manuscript Received May 29, 2008

n-Butylammonium ions intercalated in a layered aluminophosphate (AlPO-ntu) with kanemite-type structure (hereafter AlPO-kan) have been studied by IR spectroscopy and modeled with density functional theory (DFT) calculations. This joint approach clarified the local structure of the inorganic/organic interface, not yet described. The acidity of the surface hydroxyls was investigated with a finite cluster model, while the structure and the theoretical IR spectra were obtained with 3D and 2D periodic boundary conditions. In the structure here optimized, each organic ion forms three hydrogen bonds with the surface phosphate and aluminate oxygens; the theoretical frequencies, including anharmonic corrections on the main stretching modes, were compared to the experimental IR spectra. The very satisfactory agreement confirms the optimized structure and allowed all the observed peaks to be assigned, providing for the first time a clear-cut interpretation of the broad and complex absorption at 2800–1700 cm^{-1} in terms of Fermi-type resonances.

1. Introduction

Layered aluminophosphates are intermediates in the synthesis of microporous molecular sieves with channels and cavities of molecular dimensions similar to well-known zeolites.¹ CoSAPO-44 and CoAPO-44,² for instance, are formed via layered materials, and several other aluminophosphate molecular sieves, such as AlPO₄-5, AlPO₄-22, and AlPO₄-16 and the silicoaluminophosphate SAPO-35, are formed from a common lamellar material, the AlPO₄-L, during the hydrothermal treatment of a gel containing Al₂O₃, P₂O₅, SiO₂, and hexamethyleneimine, in aqueous media or in ethylene glycol.³ In addition, in the synthesis of chabazite aluminophosphates directed by morpholine, the formation of a layered prephase was also invoked.⁴

The synthesis of aluminophosphate and silicoaluminophosphate molecular sieves from layered aluminophosphates with structure similar to the hydrated silicates used in zeolite synthesis^{5–9} is relevant for the possibility to obtain novel

molecular sieves with unusual morphology and surface properties. However, until the CAL-n family of microporous silicoaluminophosphate molecular sieves was presented,¹ there were no good candidates as layered reactants, that is, lamellar aluminophosphates and silicoaluminophosphates with structures similar to the hydrated layered silicates. It is from the pioneering work of Cheng et al.,¹⁰ who reported the synthesis of the layered aluminophosphate AlPO-ntu (whose empirical formula is AlPO₂(OH)₂[NH₂(CH₂)_xCH₃], $x = 3, 5, 7$), employing amines as structure directing agents, that the perspective to obtain AlPOs and SAPOs molecular sieves using layered materials as precursors became possible.

It was proposed that the structure of AlPO-ntu is analogous to that of the siliceous kanemite, and for this reason hereafter the AlPO-ntu is called organomodified AlPO-kanemite (AlPO-kan).¹⁰ This layered material has been transformed into silico-aluminophosphates with chabazite-like structure, the CAL-1,¹¹ using hexamethyleneimine as structure directing agent. Moreover, CAL-4 with structure similar to SAPO-44, CAL-5 (AlPO-34 like structure), and CAL-3 with a levine structure have been also synthesized using AlPO-kan as precursor.¹²

* To whom correspondence should be addressed. E-mail: maurizio.cossi@mnf.unipmn.it. Tel.: 39 0131360267. Fax: 39 0131670250.
 † Università del Piemonte Orientale “A. Avogadro”.
 ‡ “Paolo Corradini” Università di Napoli “Federico II”.

- Pastore, H. O.; Coluccia, S.; Marchese, L. *Ann. Rev. Mater. Res.* **2005**, *35*, 351.
- Lee, Y. J.; Chon, H. *Microporous Mater.* **1997**, *11*, 253.
- Venkatathri, N.; Hedge, S. G.; Ramaswamy, V.; Sivasanker, S. *Microporous Mesoporous Mater.* **1998**, *23*, 277.
- (a) Vistad, Ø. B.; Akporiaye, D. E.; Lillerud, K. P. *J. Phys. Chem. B* **2001**, *105*, 12437. (b) Vistad, Ø. B.; Akporiaye, D. E.; Taulelle, F.; Lillerud, K. P. *Chem. Mater.* **2003**, *15*, 1639.
- Zones, S. I. U.S. Patent 4,676,958, 1987.
- Zones, S. I. U.S. Patent 4,689,207, 1987.
- Pál-Borbély, G.; Beyer, H. K. *Stud. Surf. Sci. Catal.* **1999**, *125*, 383.

- Salou, M.; Kiyozumi, Y.; Mizukami, F.; Nair, P.; Maeda, K.; Niwa, S. *J. Mater. Chem.* **1998**, *8*, 2125.
- Selvam, T.; Baudarapu, B.; Mabaude, G. T. P.; Toufar, H.; Schweiger, W. *Microporous Mesoporous Mater.* **2003**, *64*, 41.
- Cheng, S.; Tzeng, J.; Hsu, B. *Chem. Mater.* **1997**, *9*, 1788.
- Gieck, C.; Bisio, C.; Marchese, L.; Filinchuk, Y.; da Silva, C. E.; Pastore, H. O. *Angew. Chem., Int. Ed.* **2007**, *46*, 8895.
- Pastore, H. O.; Martins, G. A. V.; Strauss, M.; Pedroni, L. G.; Superti, G. B.; de Oliveira, E. C.; Gatti, G.; Marchese, L. *Microporous Mesoporous Mater.* **2008**, *107*, 81.

A mechanism of silicon insertion was proposed for the formation of silicoaluminophosphate molecular sieves starting from layered aluminophosphates with kanemite structure; however, neither experimental nor theoretical evidence was reported.

The interest in organomodified AlPO-kan structure is also due to the possible application in the field of polymer nanocomposites or, more generally, of the intercalation chemistry. It is well reported, in fact, that layered compounds can accommodate ions or molecules to give intercalation compounds^{13,14} suitable to be used as additives for the preparation of polymer nanocomposites.¹⁵ Thereby layered aluminophosphates can be employed as host framework for the same purposes, especially those organically modified by means of different *n*-alkylamines of increasing chain length (*n*-butylamine, *n*-dodecylamine, cetyltrimethyl-amine, etc.). These materials have the assets of a larger interlayer distance and organophilic galleries between the sheets to host either organic molecules (e.g., monomers suitable for in situ polymerization) or polymer chains.

The work of Cheng et al.¹⁰ strongly supported the definition of AlPO-kan structure with intercalated alkyl amines. IR spectra, for instance, showed peaks typical of PO_4 and AlO_4 tetrahedra connected by shared oxygens, and a strong absorption at 3580 cm^{-1} was attributed to the OH stretching of Al—OH groups alternating to $\text{P}=\text{O}^- \text{NH}_3^+ \text{R}$ (R = butyl, *n*-hexyl, *n*-octyl) ionic couples in the AlPO layers.²⁷ ^{27}Al and ^{31}P MAS NMR spectra showed that these layers are made of Q^3 -type tetrahedral atoms, assigned to $-\text{OP}(\text{OAl})_3$. In addition, the Al/P ratio was found to be unity, and the chemical formulas of the type $\text{AlPO}_3(\text{OH})_2[\text{NH}_2\text{R}]$ were determined.

Despite the breadth of the experimental data available (including X-ray powder diffraction results), they were not sufficient to fully resolve the local structure of the organic–inorganic interface. A great variety of aluminophosphates with different sheet structures, stoichiometries, and stacking sequences are found. Moreover, since AlPO-kan can be modified by intercalation of alkylamines, the interactions between the organic molecules and inorganic aluminophosphate may influence the acidity of the sites present on the surfaces and the interfacial phenomena which drive the formation of both polymer nanocomposites and AlPO molecular sieves. For these purposes, it is necessary to know more structural details of organomodified AlPO-kan, especially in relation to surface acid sites and to the interfacial interactions between inorganic and organic moieties.

Useful insights on the structure and surface properties of these materials can be provided by a combined theoretical and IR experimental study. From one side, in fact, theoretical simulations can help the experimental interpretation by providing a reliable description of hydrogen bonds in clay minerals and zeolites since these bonds strongly affect the IR data.¹⁶ From the other side, the comparison between the

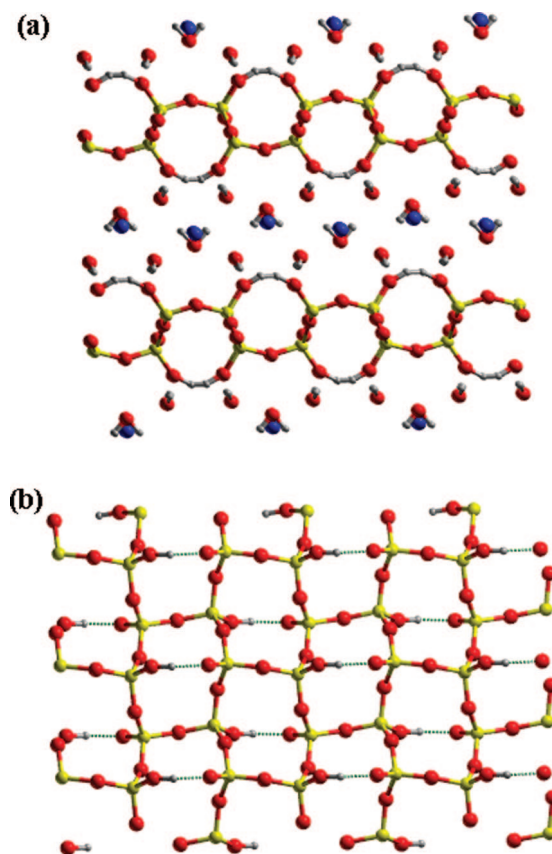


Figure 1. Supercell $2 \times 2 \times 2$ of silicate kanemite proposed by Garvie et al.¹⁷ blue, Na^+ ; red, O; yellow, Si; gray, H. (a) Front view of the layered structure; (b) top view of a single silicate sheet showing a network of silanols H-bonded to anionic siloxane ($\text{Si}-\text{O}^-$).

calculated IR spectra with the experimental ones may drive to the right choice of the model structure as well as the computational tools used (e.g., functional, basis set, and anharmonicity of the OH bond, *vide infra*).

As mentioned above, the layered AlPO-ntu structure is supposed to be similar to that of silicate kanemite whose empirical formula is $\text{NaHSi}_2\text{O}_5 \cdot 3\text{H}_2\text{O}$. The most recent reported kanemite structure¹⁷ describes a layered polysilicate in which silicate sheets alternate with hydrated Na^+ sheets; the silicate sheets contain six membered rings (6-MR) of $\text{HOSiO}_3-\text{SiO}_4$ units (Q^3 units), and the Na^+ sheet is composed of hydrated cations in distorted octahedral coordination. The six Si atoms in a ring are arranged in a distorted boat form; the orthorhombic cell (space group $Pbcn$) of Na-kanemite (Figure 1) was determined by single crystal X-ray diffraction.

2. Methods

2.1. Experimental Information. The synthesis of the *n*-butylamine AlPO-kan was performed according to the procedure already reported in the literature¹⁰ with slight modifications.¹⁸ K-exchanged AlPO-kan was prepared with the procedure reported in ref 10. IR spectra were collected at room temperature on a Bruker Equinox 55 spectrometer (resolution = 4 cm^{-1}). The samples were

(13) Hata, H.; Kobayashi, Y.; Mallouk, T. E. *Chem. Mater.* **2007**, *19*, 79.

(14) Heintz, H.; Vaia, R. A.; Krishnamoorti, R.; Farmer, B. L. *Chem. Mater.* **2007**, *19*, 59.

(15) Vaia, R. A.; Wagner, H. D. *Mater. Today* **2004**, *32*.

(16) Tosoni, S.; Doll, K.; Ugliengo, P. *Chem. Mater.* **2006**, *18*, 2135.

(17) Garvie, L. A. J.; Devouard, B.; Groy, T. L.; Camara, F.; Buseck, P. R. *Am. Mineral.* **1999**, *84*, 1170.

(18) Pastore, H. O.; de Oliveira, É.C.; Superti, G. B.; Gatti, G.; Marchese, L. *J. Phys. Chem. C* **2007**, *111*, 3116.

dispersed in deionized water and then deposited on a silicon wafer, used as a support for the powders. The silicon wafer was then kept in a properly designed IR cell equipped with KBr windows, which was permanently attached to a vacuum line allowing to make in situ treatment under controlled pressure conditions. Prior the IR analysis, the samples were evacuated at 298 K residual pressure ($<1 \times 10^{-5}$ Torr, 1 Torr = 133.33 Pa) to remove weakly adsorbed water.

2.2. Computational Details. All the calculations were performed with the density functional theory (DFT), using both the pure PBE¹⁹ and the hybrid (i.e., containing a part of the exact Hartree–Fock exchange functional) PBE0²⁰ functionals (PBE0 is sometimes referred to as PBE1PBE in the literature).

Periodic calculations were performed with CRYSTAL06,²¹ using the 6-21G(d) Gaussian-type atomic basis set enlarged with polarization functions^{22a–d} for the 3D optimizations, and a more extended double- ζ polarized basis set^{22e,f} for the 2D optimizations and frequency calculations (basis set available in Supporting Information); the PBE0 functional, which is nonstandard in CRYSTAL06, was defined by invoking the pure PBE functional, then adding 1/4 of the Hartree–Fock exchange (through the keywords HYBRID = 25 and NONLOCAL = 1, 1).

Finite cluster calculations were performed with Gaussian03²³ and the 6-31G(d) basis set with polarization functions²⁴ for the second row atoms and the LANL2DZ pseudopotentials and basis set²⁵ for Al and P.

IR spectra were simulated for the optimized periodic structure by computing harmonic frequencies with CRYSTAL06. The aluminate OH and ammonium NH stretching mode frequencies were corrected by anharmonicity, following the procedure of ref 26: the hydrogen-heavy atom distance is treated as a pure normal coordinate, decoupled from all the other modes, and the potential energy is scanned over 26 distance values (with a step of 0.02 Å) and fitted by a polynomial curve of sixth degree. The resulting one-dimensional nuclear Schrödinger equation is solved following the algorithm proposed by Lindberg.²⁷

3. Results and Discussion

3.1. Layer and Interface Structure. As stated above, the silicate kanemite cell proposed by Garvie *et al.*¹⁷ was used as a starting point to model the n-BA AlPO-kan. The silicate

- (19) (a) Perdew, J. P.; Burke, K.; Ernzerhof, M. *Phys. Rev. Lett.* **1996**, *77*, 3865. (b) Perdew, J. P.; Burke, K.; Ernzerhof, M. *Phys. Rev. Lett.* **1997**, *78*, 1396.
- (20) Adamo, C.; Barone, V. *J. Chem. Phys.* **1999**, *110*, 6158.
- (21) Saunders, V. R.; Dovesi, R.; Roetti, C.; Orlando, R.; Zicovich-Wilson, C. M.; Harrison, N. M.; Doll, K.; Civalleri, B.; Bush, I. J.; D'Arco, P.; Llunell, M. *CRYSTAL06 User's Manual*; Università di Torino: Torino, 2003.
- (22) (a) Binkley, J. S.; Pople, J. A.; Hehre, W. J. *J. Am. Chem. Soc.* **1980**, *102*, 939. (b) Gordon, M. S.; Binkley, J. S.; Pople, J. A.; Pietro, W. J.; Hehre, W. J. *J. Am. Chem. Soc.* **1982**, *104*, 2797. (c) Pietro, W. J.; Franci, M. M.; Hehre, W. J.; Defrees, D. J.; Pople, J. A.; Binkley, J. S. *J. Am. Chem. Soc.* **1982**, *104*, 5039. (d) Dobbs, K. D.; Hehre, W. J. *J. Comput. Chem.* **1987**, *8*, 880. (e) Saadoune, I.; Corà, F.; Alfredsson, M.; Catlow, R. A. *J. Phys. Chem. B* **2003**, *107*, 3012. (f) Dorner, R. W.; Deifallah, M.; Coombes, D. S.; Catlow, C. R. A.; Corà, F. *Chem. Mater.* **2007**, *19*, 2261.
- (23) Frisch, M. J.; *Gaussian03*, release C.02; Gaussian Inc.: Pittsburgh, PA, 2003.
- (24) (a) Petersson, G. A.; Al-Laham, M. A. *J. Chem. Phys.* **1991**, *94*, 6081. (b) Petersson, G. A.; Bennet, A.; Tensfeldt, T. G.; Al-Laham, M. A.; Shirley, W. A.; Mantzaris, J. *J. Chem. Phys.* **1988**, *89*, 2193.
- (25) (a) Hay, P. J.; Wadt, W. R. *J. Chem. Phys.* **1985**, *82*, 270. (b) Hay, P. J.; Wadt, W. R. *J. Chem. Phys.* **1985**, *82*, 299. (c) Hay, P. J.; Wadt, W. R. *J. Chem. Phys.* **1985**, *82*, 284.
- (26) Ugliengo, P. ANHARM—A program to solve monodimensional nuclear Schrödinger equation; 1989, unpublished.
- (27) Lindberg, B. *J. Chem. Phys.* **1998**, *88*, 3805.

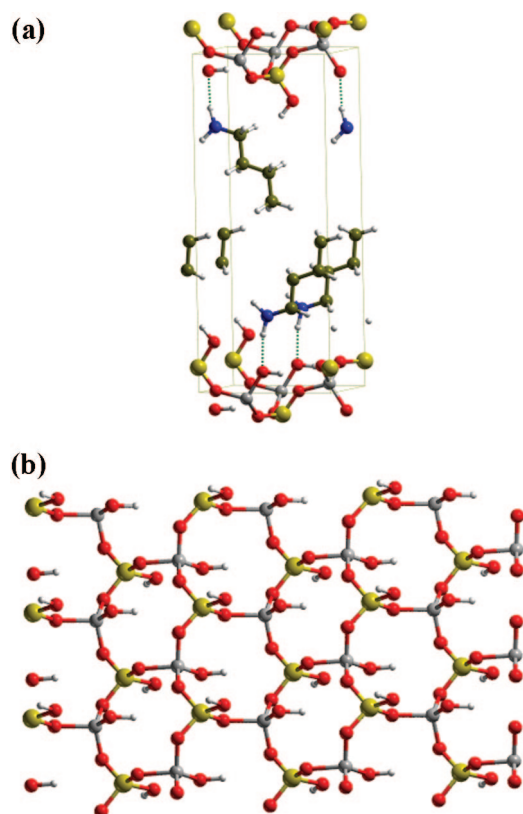


Figure 2. (a) Unit cell of *Pmn*₂₁ model optimized for butylamine AlPO-kan with 3D periodic boundary conditions: blue, N; green, C; red, O; yellow, Si; gray, H; (b) top view of a single AlPO-kan sheet where each tetrahedron is terminated by Al–OH or P–OH.

kanemite is formed by rings of 6 silicon atoms (6-MR) connected by oxygens: in the AlPO-kan the silicon atoms are substituted by alternated Al and P atoms. First, the inorganic layers were intercalated by butylamine molecules (with the same stoichiometry as the hydrated Na ions in the Na-kanemite), with a periodic constant along the *z* axis of 1.8 nm, in agreement with the X-ray powder diffraction pattern (data not shown for brevity), which exhibits the basal plane peak at $2\theta = 4.84^\circ$. In this model, all the phosphate and aluminate groups are protonated, and the 3D structure belongs to the orthorhombic *Pmn*₂₁ group, in analogy with the silicate kanemite. Figure 2 shows the structure optimized at the PBE0/6-21G(d) level.

However, the IR spectra (vide infra) indicate that *n*-butylamine is protonated as a consequence of an acid–base reaction with some of the surface hydroxyl groups. Cheng *et al.*¹⁰ detected Al–OH groups on the surface even in the presence of butylammonium ions, thus suggesting that phosphate is more acidic and that protonated amines act as counter-ions of anionic P–O[−] groups. Following this hypothesis, another geometry optimization was performed, at the same level and with the same symmetry group as above, intercalating butylammonium ions and deprotonating all the phosphate groups on the surface. This optimization led to a structure where the energy minimum is 38.4 kcal per mole of butylammonium lower than that with neutral amines, confirming that the acid–base reaction between the surface hydroxyls and the amino groups is exothermic. The structure belongs to the *Pmn*₂₁ group, with parameters *a* =

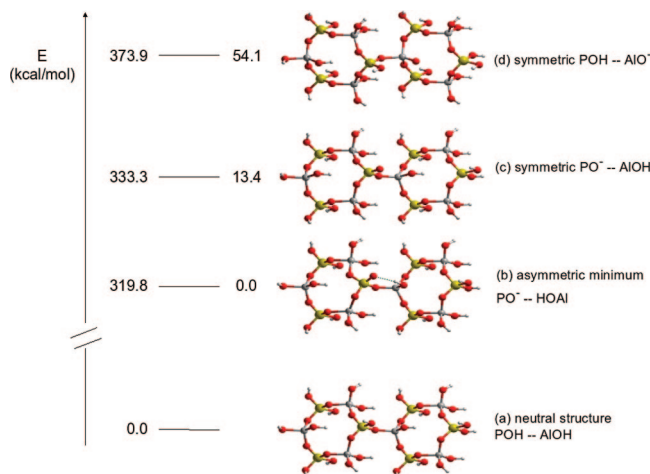


Figure 3. Structure of neutral and anionic clusters optimized in vacuo at the PBE0/LANL2DZ/6-31G(d) level; in the first column are the deprotonation energies (kcal/mol) of the various cations, and in the second column are their relative energies (kcal/mol).

7.396 \AA , $b = 5.475 \text{ \AA}$, and $c = 18.000 \text{ \AA}$ (the c parameter was held frozen during the optimization).

The relative acidity of the Al–OH and P–OH groups on the AlPO-kan surface was further investigated on a cluster model, removing some of the symmetry constraints: an $\text{Al}_6\text{P}_6\text{O}_{35}\text{H}_{22}$ cluster was cut out of the neutral optimized layer (Figure 3a), including two 6-member rings and saturating all the dangling bonds with hydrogens. The cluster was reoptimized using Gaussian03 with the PBE0 functional and a basis set including LANL2DZ pseudopotentials and basis on Al and P, and 6-31G(d) on the other atoms; then two anions, obtained by extracting a hydrogen from the P–OH and Al–OH groups, respectively (Figure 3c,d), were optimized keeping the local symmetry as in the 3D structure. Finally, another anion was optimized removing the symmetry constraints on the Al–OH and P–OH groups and allowing the formation of an intramolecular hydrogen bond (Figure 3b). The optimized structures, along with their relative energies, are reported in Figure 3.

The cluster calculations confirmed that the phosphate group is much more acidic than aluminate, and it is likely to provide the proton to form the butylammonium ion. It is important to note that by removing the local symmetry the energy lowers markedly, thanks to the formation of intramolecular hydrogen bonds: since in the actual system the local structure of the surface groups is likely to be altered by the organic counterions, a more reliable description can be obtained with a lower symmetry group, allowing a more favorable rearrangement of the interface. This prompted us to repeat the periodic optimization on a single slab of n-BA AlPO-kan removing any point symmetry constraints.

Then a 2D slab of butylammonium AlPO-kan was optimized with CRYSTAL06 at the PBE0 level with the extended basis set cited in the Computational Details section: a monolayer of organic ions was present on both slab faces. The optimized structure belongs to the P_1 group, and the cell parameters are $a = 15.383 \text{ \AA}$, $b = 4.832 \text{ \AA}$, and $\gamma = 90.0^\circ$: the resulting structure is depicted in Figure 4. With respect to the 3D $Pmn2_1$ structure the ions are closer to the

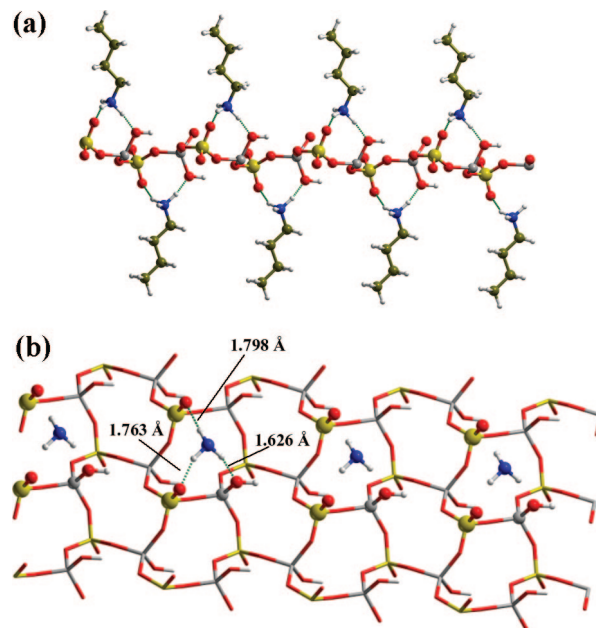


Figure 4. n-BA AlPO-kan optimized at PBE0/6-21G(d) level (see text) and bidimensional periodic boundary conditions. (a) Side view; (b) top view (for the sake of clarity, the carbon atoms have been omitted, and only the atoms involved in H-bonds are highlighted).

surface, and three hydrogen bonds are established between the ammonium and the surface oxygens (H–O distances 1.626 , 1.763 , 1.798 \AA). As indicated in Figure 4b, the shortest (and strongest) H-bond is formed with the Al–OH oxygen, which is somehow unexpected: however, each PO_4^{3-} group forms two H-bonds with ammonium hydrogens so that the effect of the net charge is reduced. The intermolecular H-bond found in the cluster structure between Al–OH and one of the phosphates is lost, in favor of stronger interactions with the ammonium hydrogens: on the other hand, the Al–OH hydrogen weakly binds to one of the Al–O–P oxygens of the adjacent ring. The organic molecules are roughly perpendicular to the slab, in order to optimize the H-bonding with the surface oxygens and the side-to-side intermolecular interactions.

The reliability of this structure can be tested by comparing its vibrational spectrum, computed at the same level used for the geometry optimization, with the experimental IR spectrum, as detailed in the following section.

3.2. Experimental and Simulated IR Spectra. Figure 5 shows the experimental IR spectrum of n-BA AlPO-kan compared to that of K^+ -exchanged AlPO-kan to highlight the vibrational features of the butylammonium ions. The n-BA AlPO-kan spectrum shows a narrow band at 3580 cm^{-1} , assigned to hydroxyl stretching of Al–OH groups, and several bands in the 3400 – 1200 cm^{-1} region, which are due to the vibrational modes of n-BA ions, since they are not detected in the K^+ -exchanged sample. A weak band is found at 3250 cm^{-1} , which is removed upon heating at low temperature (120 – 150°C) under vacuum, and it is attributed to *n*-butylammonium ions weakly adsorbed on the external AlPO surface.

An interesting very large and complex absorption, not assigned in the literature yet, is detected in the 2800 – 1700 cm^{-1} region, with maxima observed at 2766 , 2673 , 2523

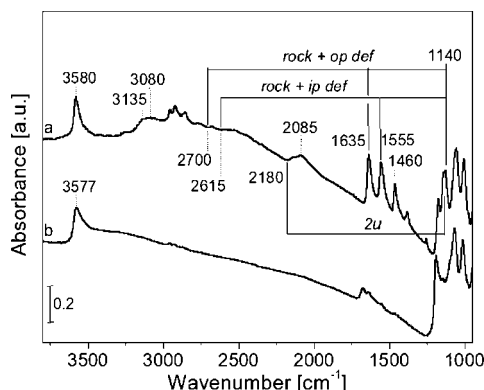


Figure 5. IR spectra of n-BA AlPO-kan (a) and K-AlPO-kan (b). The vibrational modes which give origin of Fermi resonances are evidenced (op def, out-of-phase deformation; ip def, in-phase deformation).

(not indicated in Figure 5), and 2085 cm^{-1} . Several bands are found in the $1700\text{--}1200\text{ cm}^{-1}$ region, and narrow absorptions at 1172 , 1140 , 1055 , and 1005 cm^{-1} are present in the low wavenumber region.

In the spectrum of K-AlPO-kan (curve b), the stretching mode of Al-OH species is found at 3577 cm^{-1} . An exceedingly low amount of n-BA ions is still observed in this sample, as witnessed by the presence of weak bands in the $3150\text{--}2800\text{ cm}^{-1}$ and $1650\text{--}200\text{ cm}^{-1}$ regions, attributed to stretching and deformation modes of NH_3^+ , CH_3 , and CH_2 groups. The presence of a broad absorption in the $3450\text{--}3150\text{ cm}^{-1}$ range, accompanied by a weak band at 1670 cm^{-1} (not observed in the n-BA AlPO-kan), indicates that this sample contains water molecules bound to K^+ ions. In the $1200\text{--}950\text{ cm}^{-1}$ range, the spectrum of K-AlPO-kan sample shows the presence of well defined absorptions at 1190 , 1145 (very weak), 1068 , and 1010 cm^{-1} .

As stated in the Introduction, the interpretation of IR spectra can be refined by comparison with theoretical models, which provide useful (and in some cases unique) information on the atomic structure of the organic/inorganic interface. The harmonic frequencies computed for the 2D slab at the PBE0 level with the extended basis set (see Computational Details section) are listed in Table 1, along with the experimental absorptions; for some stretching modes the anharmonic corrected wavenumbers, computed as explained in the Computational Details section, are also reported.

The Al-OH stretching mode harmonic frequency is computed at 3902 cm^{-1} , corrected to 3736 cm^{-1} by anharmonicity: the highest frequency experimental peak (3580 cm^{-1}) can be attributed to this mode.

The NH_3^+ harmonic stretching modes (with all the hydrogens engaged in H-bonds to surface oxygens) are computed in the $2811\text{--}133\text{ cm}^{-1}$ region. The analysis of the normal modes shows that the H-bond directed toward the Al-OH group is fairly decoupled, whereas the two other H-bonds (pointing to the P-O groups) are strongly coupled. As a consequence, the anharmonic correction is expected to be more reliable for the former motion than for the latter ones (since in our procedure the anharmonicity is calculated by moving each hydrogen separately). However, using the corrections computed for the three ammonium hydrogens, the N-H-O-Al stretching frequency is 2442 cm^{-1} , the out-

Table 1. Computed Harmonic and Anharmonic Vibrational Frequencies (cm^{-1}) for the 2D n-BA AlPO-kan Slab with a Single Layer of Butylammonium Ions, Compared to the Experimental IR Absorptions

groups	vibrational modes	computed harmonic frequencies (cm^{-1})	computed frequencies corrected for anharmonicity (cm^{-1})	experimental frequencies (cm^{-1})
Al-OH NH_3^+	ν_{OH}	3902	3736	3580
	$\nu_{\text{NH}\cdots\text{O-P}}$ (in phase)	3133	2819	3135
	$\nu_{\text{NH}\cdots\text{O-P}}$ (out of phase)	3067	2753	3080
	$\nu_{\text{NH}\cdots\text{O-Al}}$	2811	2442	2800–1700
	out-of-phase def.	1725		1635
	in-phase def.	1650		1555
	rocking	1129		1140
	CH ₃ , CH ₂ stretchings	3047–3043	2937–2933	2960–2860
	CH ₂ scissoring	1527		1460
	CH ₂ wagging	1443		1390
CH ₃	in-phase def.	1426		1380
	CH ₂ twisting	1344–1307		1256

of-phase combination of the two N-H-O-P stretchings falls at 2753 cm^{-1} , and the in-phase combination is at 2819 cm^{-1} .

In the experimental spectrum two absorptions at 3080 and 3135 cm^{-1} are likely to be associated to two stretching modes of ammonium hydrogens bound to the surface oxygens: the calculation underestimates the frequencies of both the N-H-O-P stretching modes by about 300 cm^{-1} . The most likely explanation of this discrepancy is that in the optimized structure the ammonium group is too close to the surface, making the H-bonds stronger than in the real structure. As described above, the IR spectrum is simulated using a 2D periodic slab, with a single organic monolayer above and below the inorganic sheet (Figure 4): this structure has the correct periodicity along the two (a and b) surface axes; however, it does not describe the interactions with the other organic layers along the *c* axis. Such interactions are likely to attract the butylammonium molecules slightly apart from the inorganic surface, and this may explain qualitatively the discrepancy between the theoretical and observed frequencies of the NH stretchings.

On the other hand, since the crystallographic AlPO-kan 3D structure has not been resolved yet, the slab structure presented above is the most accurate model of the local structure that we can use (in any 3D periodic model, the position of the organic molecules depends on the imposed global symmetry, while in the slab the butylammonium was allowed to relax to the most favorable position).

The CH₃ and CH₂ harmonic stretching modes are computed in the $3047\text{--}3043\text{ cm}^{-1}$ region; as above, since the C-H motions are strongly coupled, the anharmonic corrections cannot be predicted with precision. However, these corrections are estimated to be $100\text{--}110\text{ cm}^{-1}$ (by computing the anharmonic correction for a single CH₃ stretching). The overall computed band is then $2937\text{--}2933\text{ cm}^{-1}$, in good agreement with the observed band at $2860\text{--}2960\text{ cm}^{-1}$.

The harmonic frequencies of deformation modes are computed at 1527 (CH₂ scissoring) and $1344\text{--}1307\text{ cm}^{-1}$ (CH₂ twisting): these modes are associated to the experimental peaks at 1460 and 1256 cm^{-1} , respectively. The

experimental absorptions at 1390 and 1380 cm^{-1} can be assigned to CH_2 wagging (computed wavenumber 1443 cm^{-1}) and to in-phase CH_3 deformation (computed band at 1426 cm^{-1}), respectively.

The NH_3^+ deformation modes have harmonic frequencies at 1725, 1650, and 1129 cm^{-1} , attributed to the out-of-phase and the in-phase combinations and the NH_3^+ rocking motion, respectively. By comparison, these modes are assigned to the experimental absorptions at 1635, 1555, and 1140 cm^{-1} , respectively: as expected, the computed (harmonic) frequencies are slightly overestimated with respect to the experimental ones.

As for the complex band structure observed in the 1700–2800 cm^{-1} region, these features can be explained as due to Fermi resonances between the ammonium proton stretching computed at 2442 cm^{-1} ($\text{NH}\cdots\text{OAl}$) and combinations and overtones of NH_3^+ deformations. The band of the 1140 cm^{-1} may combine (in harmonic approximation) with the deformation modes at 1635 and 1555 cm^{-1} to give bands at 2775 and 2695 cm^{-1} , respectively; in addition, its second harmonic should fall at 2280 cm^{-1} . These bands may give Fermi resonances with the strong band of the $\text{NH}\cdots\text{OAl}$ absorbing at 2800–1700 cm^{-1} , generating three Ewans windows; three minima are in fact detected at 2700, 2615, and 2180 cm^{-1} . It is now clear that the bands in the 2800–1700 cm^{-1} region are only apparent maxima and that the real position of the proton ($\text{NH}\cdots\text{OAl}$) stretching, the computed value being at 2442 cm^{-1} , cannot be determined with precision. However, if the relative intensity of the maxima in this region is considered, the baricenter of the $\text{NH}\cdots\text{OAl}$ stretching band should be close to the Ewans window at 2180 cm^{-1} .

The analysis of the n-BA AlPO-kan IR spectrum in a region which had not been described previously strongly supports the structure described above of the inorganic–organic interface. To the author's opinion, the knowledge of such local structure is the first necessary information to solve completely the 2D AlPO-ntu structure which has not been hitherto determined.

4. Conclusions

The structure of the aluminophosphate layers, the acidity of the surface sites, and the interactions with intercalated butylammonium ions in n-BA AlPO-kan have been investigated through a combination of IR spectroscopy and computational analysis.

Starting from the silicate kanemite geometry, two 3D periodic structures have been optimized at the DFT level within the $Pmn2_1$ symmetry group, with butylamine and

butylammonium ions intercalated, respectively: the structure with butylammonium ions (and deprotonated phosphate groups on the surface) resulted in being much more stable, indicating that an acid–base reaction takes place between the surface hydroxyls and the organic molecules. The relative acidity of aluminate and phosphate surface groups was further investigated with a cluster model, confirming that the phosphate is markedly more acidic. Moreover, it was shown that the removal of some symmetry constraints allowed a much more convenient arrangement for the organic layer to be found.

A 2D periodic structure was subsequently optimized with the P_1 symmetry group, including a single slab of AlPO-kan and two layers of butylammonium ions: in this structure each organic ion is H-bonded to three oxygens on the surface (one from $\text{Al}-\text{OH}$, two from $\text{P}-\text{O}$ groups). The reliability of this geometry was verified by computing harmonic and (for some modes) anharmonic vibrational frequencies, and their comparison with the experimental IR spectrum. This also allowed for the first time the experimental spectrum to be solved by assigning all the main absorptions: in particular, the complex band in the 2800–1700 cm^{-1} region has been described in terms of Fermi resonances between the $\text{NH}\cdots\text{O}-\text{Al}$ stretching (whose anharmonic frequency is computed at 2442 cm^{-1}) and overtones and combinations of NH_3^+ deformation modes.

The good agreement between the experimental and calculated frequencies confirmed the reliability of the optimized local structure of the organic/inorganic interface and provided relevant information for future powder XRD analysis of the crystal structure.

Acknowledgment. We are very grateful to Prof. H.O. Pastore and Mr. M. Strauss (University of Campinas, Brazil) for providing n-BA and K^+ -exchanged AlPO-kanemite samples. One of the reviewers is gratefully acknowledged for valuable comments and suggestions, which have contributed to improve the quality of the paper substantially. M.D.A. and G.T. thank the “Fondazione Cassa di Risparmio di Torino” (FCRT) for the grants supporting their scientific activity. The authors acknowledge the European Commission for financial support (Stabilight STREP project).

Supporting Information Available: Extended basis set cited in the Computational Details section (TXT); the CIF files of the optimized periodic structures of AlPO-butylamine (3D structure), AlPO-butylammonium (3D structure), AlPO-butylammonium (2D slab); and the normal mode definition in terms of atomic Cartesian coordinates, as reported in the CRYSTAL06 output file (TXT). This information is available free of charge via the Internet at <http://pubs.acs.org>.

CM8009594